ACS APPLIED MATERIALS & INTERFACES

Research Article

www.acsami.org

Binding of HIV-1 gp120 Glycoprotein to Silica Nanoparticles Modified with CD4 Glycoprotein and CD4 Peptide Fragments

Kai Cheng, Kheireddine El-Boubbou, and Christopher C. Landry*

Department of Chemistry, University of Vermont, 82 University Place, Burlington, Vermont 05405, United States

Supporting Information

ABSTRACT: An important step in human immunodeficiency virus infection involves the interaction between the viral envelope glycoprotein gp120 and the human host cell surface receptor CD4. Herein, we describe a CD4-functionalized mesoporous silica-based system to selectively capture HIV-gp120 with high binding efficiency. Using a protection−deprotection strategy developed recently by our group, the external surface of the mesoporous particles was selectively functionalized with soluble CD4 ("sCD4") or an 18-peptide fragment mimicking the gp120 binding region. Confocal microscopy confirmed the CD4 locations and showed that the internal pores can be made accessible after external modification in a controlled manner. An evaluation of the ability of an 18-peptide CD4 fragment versus amide-immobilized sCD4 and sCD4 immobilized through its glycosidic group indicated that while all peptides were selective, the latter method was clearly best, with nearly complete removal of whole gp120 from solution. This study shows, for the first time, that sCD4 bound to mesoporous silica particles actively recognizes and retains high binding affinity for HIV-gp120. It is anticipated that, by proper modification of the accessible internal pores, our methodology can be adopted to develop porous platforms for HIV diagnosis, imaging, drug delivery, and vaccine development.

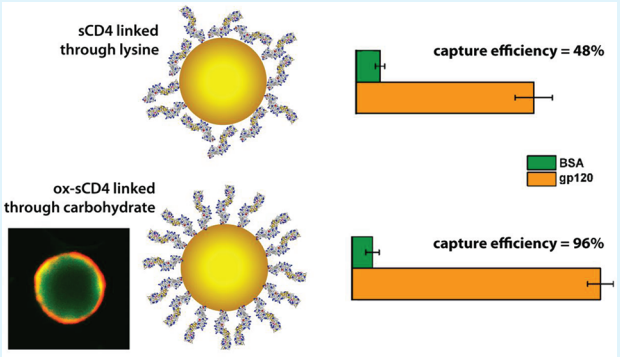

KEYWORDS: *biomedical applications, protein binding, silica, surface modification, porous materials*

INTRODUCTION

The ease with which silica surfaces can be functionalized has led to the development of multifunctional silica-based materials for various diagnostic and therapeutic biomedical applications. In particular, considerable effort has been directed towards developing mesoporous silica spheres immobilized with biomolecules (i.e., glycoproteins, peptides or antibodies), leading to impressive developments in medical diagnostics,[1] biomolecular targeting,[2−4] cellular labeling,[5] imaging,[6,7] drug delivery,[8−10] and biosensing/bioseparation processes.[11−13] Related materials such as composite nanomaterials, magnetic particles, and macroporous microbeads have been successfully used to capture and separate glycosylated peptides/proteins.[14−16] Moreover, mesoporous silica has been utilized for the selective enrichment of glycopeptides from biological samples.[17−19] One unique opportunity is to develop novel particle-based detection methods to improve upon the time-consuming biochemical methods of ELISA, western blots, and PCR amplification.[20,21] For example, only a few nanoparticle-based immunoassay methods for detection of HIV-1 antigens, particularly the capsid (p24), have been reported.[22−24] However, to the best of our knowledge, there are no reports on mesoporous silica materials functionalized with glycoproteins for targeting the HIV-gp120 antigen and potentially the HIV virus itself.

A major mechanism of HIV infection involves the interaction of the exterior viral glycoprotein envelope gp120 with the transmembrane receptor glycoprotein CD4, which is expressed predominantly on T lymphocytes.[25−27] The gp120-CD4 interaction has been thoroughly investigated,[28] and the crystal structures of gp120 binding to soluble CD4 (sCD4) and a CD4-induced (CD4i) antibody have been reported.[29] It has been shown after gp120 binds CD4 on target cells, conformational changes are triggered in gp120 that allow a highly conserved, hidden bridging sheet to become exposed, allowing it to bind to one of two chemokine receptors (CXCR4 or CCR5)[30−32] that mediate viral entry to the host. The exposed location of the gp120 glycoprotein on the virus renders it potentially vulnerable to neutralizing antibodies. However, the elicitation of broadly reactive neutralizing antibodies is inefficient and fails to neutralize the virus.[33] Accordingly, chemical conjugates of sCD4 with toxins, or with antibodies that activate cytotoxic T cells in vivo can be used to direct selective killing of HIV-infected cells. For instance, the potent and broad neutralizing activity of the bifunctional recombinant HIV-1 neutralizing protein sCD4-17b against genetically diverse HIV-1 primary isolates highlights the potential for antiviral approaches to combat HIV infection.[34] Porous particles modified with sCD4 or sCD4 mimics could function

Received: September 22, 2011
Accepted: November 25, 2011
Published: November 25, 2011

Scheme 1. Summary of the Synthetic Strategies for Covalent Immobilization of Peptide or Glycoprotein on APMS[a]

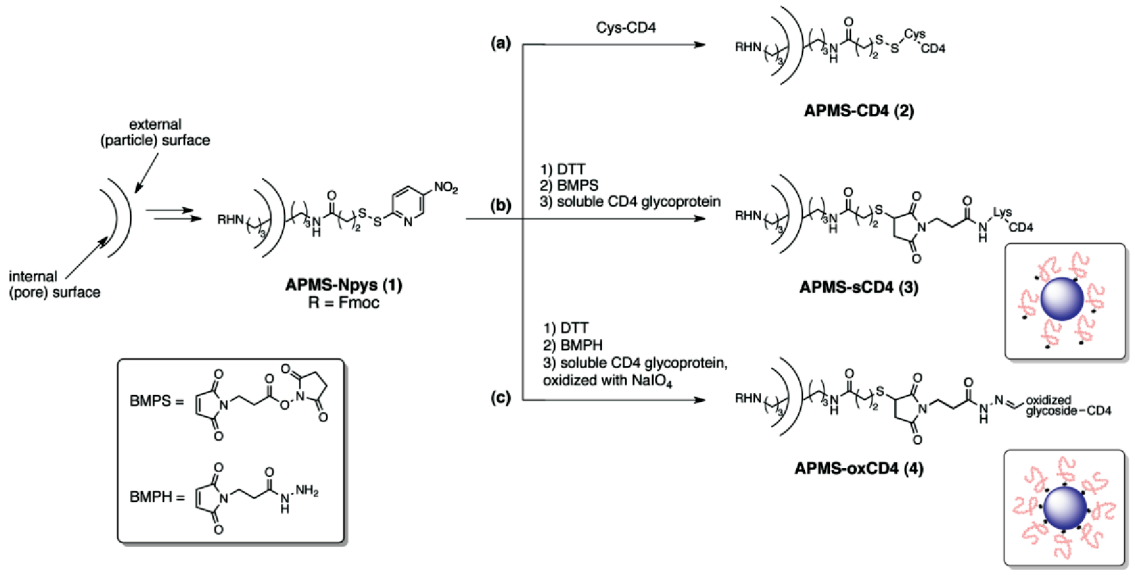

[a]DTT = dithiothreitol; BMPS = N-[β-maleimidopropionic acid]-succinimide ester; BMPH = N-[β-maleimidopropionic acid]-hydrazide.

as "Trojan horses" in this capacity, because the external surface can be optimized for binding while at the same time the pores can be loaded with an antiviral agent. For the development of particle-based HIV detection and therapeutic methods, it is important to identify the proper surface linkage and orientation required to retain optimum binding affinity.

Because of their large internal surface area and pore volume, tunable pore size, uniform shape and biocompatibility, mesoporous silica offers unique advantages in the development of a cellular targeting device. However, the successful use of such particles often requires selective modification of internal and external surfaces, which can be challenging.[35−38] Recently, we reported a new and simple strategy by which APMS particles can be differentially functionalized through diffusion-based amine deprotection,[39] resulting in particles with functionalized biomolecules exposed solely on their external particle surfaces and amines distributed inside the pores. We observed that reactions within the pores were spatially confined and a molecular size exclusion effect was produced by the diffusion of reactants and products physically constrained in the pores. Using this procedure, we designed and prepared APMS with various CD4 fragments immobilized on its external surface and confirmed their location using fluorescence confocal scanning laser microscopy (CSLM). The processes of the immobilization within the mesoporous silica were quantitatively monitored via photometric measurements. The accessibilities of the peptides and proteins to the binding sites were evaluated. To gain insight into the immobilization behaviors of the peptides and proteins, we used a Langmuir isotherm model to analyze the equilibrium binding data. Finally, we showed, for the first time, that sCD4 glycoproteins bound to the silica surface actively recognize HIV-gp120 and retained its high binding affinity, removing the gp120 from solution.

RESULTS AND DISCUSSION

Overall Strategy. APMS were the type of disordered mesoporous silica particles used in this study, mainly due to their porosity, spherical morphology, and optical transparency in the UV/visible spectrum.[40−42] They are easily and rapidly synthesized in multigram scale in less than 2 h, with good control over pore diameter and particle diameter.[40−44] Our overall synthetic strategy is shown in Scheme 1. Essentially, we set out to prepare several types of modified APMS particles for binding studies with whole gp120 glycoprotein, to determine the factors affecting successful binding at the particle surface. We prepared APMS modified with several peptide fragments of various lengths that corresponded to the gp120 binding region, and we also prepared APMS modified with whole soluble CD4 (sCD4), using two methods to attach the protein to the particle surface. Functionalized APMS particles were thoroughly characterized by a variety of techniques, including scanning electron microscopy (SEM), thermogravimetric analysis (TGA), FTIR spectroscopy, and N_2 physisorption.

Controlled Modification of Porous Silica Particles with Peptide Fragments. To insure that the CD4 fragments were immobilized only on the external surface of the porous particles, differential functionalization via an Fmoc protection/deprotection method was employed. As studied extensively by our group and others, Fmoc protection of amines is useful for the controlled-differential functionalization of mesoporous silicas.[45] Briefly, Fmoc-modified aminopropyltriethoxysilane (Fmoc-APTES) was reacted with APMS to produce a material with both pore and external surfaces modified with protected amines, followed by exposure of the resulting solid to 5% piperidine in DMF to initiate deprotection. Quantitative analysis of the deprotection process is readily available from UV/Vis spectroscopy of the fluorenyl deprotection product. Plotting the extent of deprotection versus time for the samples in these experiments showed the typical sigmoidal curve found for mesoporous samples, with a brief initial "lag time" (t_{lag}) of 74 min followed by a rapid "burst phase" when the majority of the amines within the pores were deprotected. We optimized the time required for external surface modification by varying the exposure of the solids to the piperidine solution. A dramatic increase in the surface area, pore volume, and pore diameter as measured by N_2 physisorption was clearly observed, as the

dx.doi.org/10.1021/am2013008 | ACS Appl. Mater. Interfaces 2012, 4, 235−243

pores that had been blocked with Fmoc groups were "reopened" following deprotection. For example, when the deprotection time was 40 min, the deprotection reaction was exclusively restricted to the external surfaces of the particles. When the time was increased to 120 min, additional deprotection occurred near the pore entrances. After 360 min, at least 60% of the Fmoc groups had been removed and the blocked pores were reopened.

Because all of the free amines in the solid that was deprotected for 40 min were located on the external surface, the second synthetic step of reacting deprotected amines with the crosslinking molecule 3-nitro-2-pyridyl-disulfanyl-propanoic acid (Npys-PA) could be performed nearly quantitatively. Of the deprotected amines, approximately 97% were reacted with Npys-PA as determined by TGA. Moreover, to show that the internal pore volume of the modified particles could still be made accessible for future molecular exchange or drug loading, the APMS-Npys was exposed to the piperidine solution for a full 24 h to completely deprotect the solid. Under these conditions, the porosity recovered to nearly the initial conditions (SA_{BET} = 739 m^2/g; V_{pore} = 0.358 m^3/g; d_{pore} = 2.6 nm), showing that immobilization of Npys-PA did not result in the blockage of the pore entrances.

On the basis of the structure of CD4 with gp120 bound at its active site, several short peptide sequences of the CD4 glycoprotein that are primarily responsible for the interaction have been identified. The loop corresponding to residues 35-51 of the first domain of CD4 is thought to be very critical for gp120 binding,[26,46,47] because it contains residues such as Lys35, Phe43, Leu44, Lys46, and Gly47, which are involved in direct interaction with gp120. In particular, Phe43, which is located in the fourth position of a β-turn of the loop pointing away from the surrounding residues, fits a hydrophobic binding pocket of gp120 and is thought to be particularly important for gp120 binding; this residue alone contributes 23% of the total interaction contact with gp120.[34] The Npys groups on our silica beads provided a protected and activated disulfide that could be used to couple with cysteine-modified peptide fragments. Several peptide fragments were prepared by standard solid-phase peptide synthesis procedures, derived from the crucial binding loop and modified with a cysteine at either the *N*- or *C*-terminus to facilitate disulfide bond formation with the particle surface: (1) the entire sequence of peptides 35-51 (18 peptides, called "18-CD4" in our studies); (2) residues 42-44, containing the crucial Phe43 residue ("4-CD4"); (3) peptides 35-51 with four alanine residues incorporated at both the *N*- and *C*-termini in addition to the cysteine ("26-CD4"). No additional cysteines were present in the fragments themselves, providing a convenient way to anchor the fragments to the APMS surface while avoiding interactions within the fragments themselves. All the above reactions exhibit well-behaved kinetics and can be easily monitored with conventional spectroscopic methods.[48] The degree of the loading of the CD4 peptides on APMS was easily monitored by the measurement of *p*-nitropyridinethiol release using UV/Vis spectroscopy.

Characterization of Peptide-Functionalized Particles with FTIR Spectroscopy. Although the FTIR spectrum of particles containing protected amines showed prominent peaks at 1701 and 1546 cm^{-1} because of the carbamate linkage of Fmoc (Figure 1, detailed peak assignments in the Supporting Information), the absence of these bands after deprotection indicated Fmoc cleavage. After modification with Npys, characteristic peaks due to the new functional group were found at 1590 and 1571 cm^{-1} (aromatic ring stretch) and 1348 cm^{-1} (NO_2 symmetric stretch), which closely match the corresponding peaks in same region of the spectrum of pure Npys. The immobilization of CD4 fragments on APMS-Npys was also confirmed by the absence of a very strong peak at 1348 cm^{-1} after cysteine-modified peptides had reacted with APMS-Npys. Finally, the conformational behavior of the CD4 peptides attached to the solid support was essentially the same as that observed in the pure phase. The results indicate that all the peptides mainly exhibit an essentially unordered conformation (random coil), characterized by the existence of strong single bands at ~3300 and 1660 cm^{-1}.[49−51] The similarities between the spectra of the peptides before and after immobilization indicated that they retained their solution-phase structures.

Visual Analysis of CD4 Location by Confocal Microscopy. CSLM was used to insure that the CD4 fragments were selectively immobilized on the exterior surface of APMS. CD4 peptides labeled with Alexa-568 were incorpo-

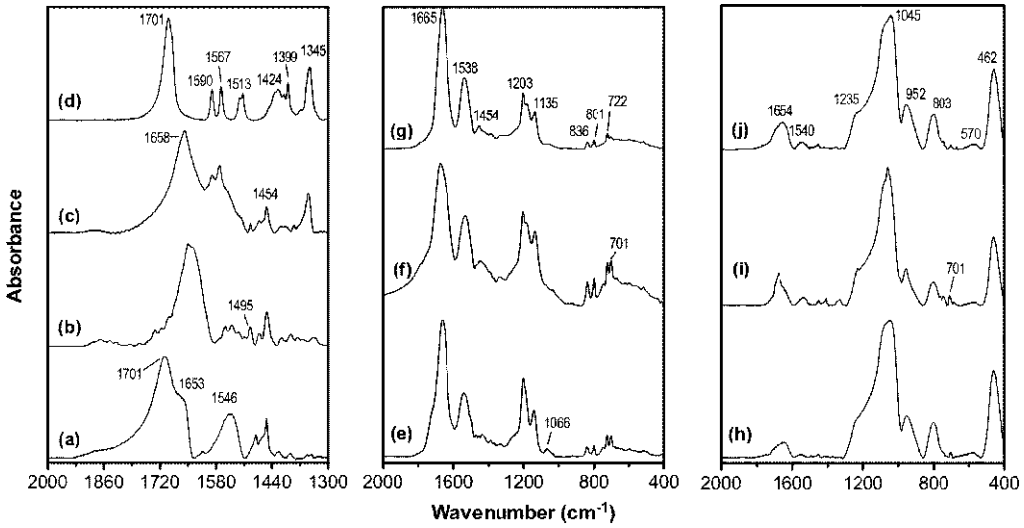

Figure 1. FTIR spectra. Left: (a) APMS-Fmoc, (b) APMS-Fmoc after deprotection for 40 min, (c) APMS-Npys, and (d) Npys-PA. Center: (e) 4-CD4, (f) 18-CD4, (g) 26-CD4. Right: (h) APMS-4-CD4, (i) APMS-18-CD4, and (j) APMS-26-CD4 in the regions of 400−2000 cm^{-1}.

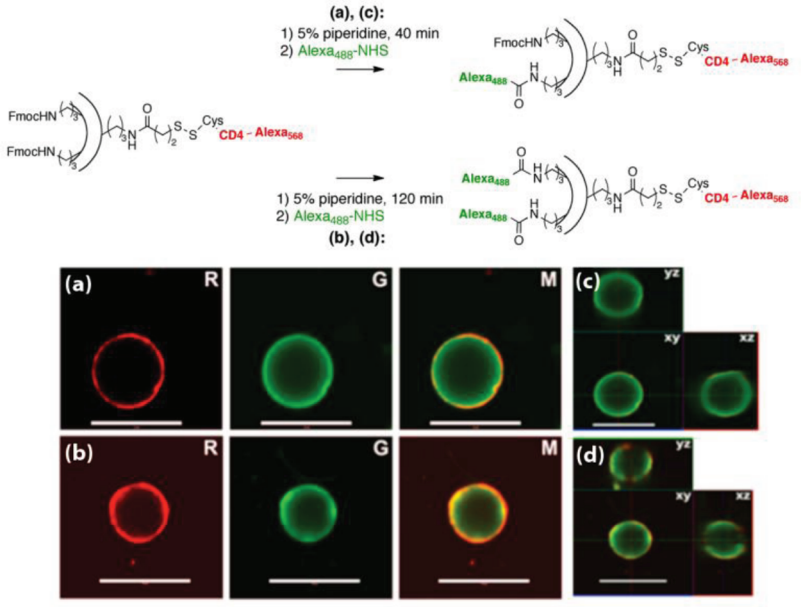

Figure 2. Colocalization analysis of Alexa-568- and Alexa-488-labeled, CD4-functionalized APMS. In this construction, Alexa-488 appears green and Alexa-568 appears red. R, G, and M represent red, green, and merged channels, respectively; (a) after 40 min, (b) after 120 min of 5 % piperidine Fmoc deprotection. Orthogonal presentation of a stack of colocalized dual channel CSLM images of the Alexa-568 and Alexa-488 -labeled CD4 functionalized APMS, (c) after 40 min, (d) after 120 min in the simultaneous view of *xy*, *xz*, and *yz* planes (*z* direction is in/out of the page). (Scale bar: 10 μm).

rated covalently onto the external surfaces by the methodology described above. Then, following exhaustive deprotection to remove Fmoc located inside the pores, the solid was reacted with Alexa-488 succinimidyl ester. In the resulting dual-channel fluorescence CSLM images of this material (Figure 2), the response from Alexa-568 was false-colored red and Alexa-488 was green. The presence of well-defined rings in the red (CD4) channel indicated that the peptides were located on the external surfaces of the silica particles. The brightness and thickness of the ring corresponded to the amount of peptides bound to the particle surface and the penetrating depth of the peptides during immobilization, respectively. The green channel (free amines) showed that deprotected amines were located mainly within the particle; interestingly, the brightness of the green fluorescence was not homogeneous within the particles' interior. This is could be due to the increased amount of silica through which the fluorescence travels in creating the image, but it also appears that there were fewer free amines located in the interior of the particles as opposed to near the surface. It is likely that a larger density of the initial surface functionalization occurred near the openings of pore channels rather than in the center of the particles. At longer deprotection times, there appeared to be less green dye present and a wider and more diffuse red ring, indicating that some peptides were bound near the pore entrances, blocking access to the pores. In addition, a small number of free amines were identified on the external surface of the particles (yellow in the merged images), confirming that peptide coverage on the surface was not complete. CSLM optically sections the silica spheres to visualize internal details by providing a view though the center of the spheres in the *xy* plane, and in the *xz* and *yz* planes through the image stack, and thus visibly provides the locations of functionalized dye-labeled CD4 within the silica spheres. Several views of the samples at different angles clearly exhibited that only surfaces of the spherical particles had been modified and there was no evidence of the immobilization of the Alexa568-peptides inside the pores.

Structural Features of sCD4 Glycoprotein Relevant to Binding at Particle Surfaces. With confidence that the deprotection strategy employed above allowed molecules to be selectively attached to the external surfaces of the particles, we moved on to investigate the possibility of attaching a recombinant human soluble form of CD4 (sCD4) on the external surface of APMS to bind HIV-1 gp120. sCD4 is a 363-amino-acid glycoprotein (~45 kDa) composed of four extracellular immunoglobulin-like domains (D1−D4). It is a truncated form of the extracellular human-T cell CD4 co-receptor produced by transfection of insect cells with vectors encoding forms of the CD4 gene.[26,52] D1 of sCD4, the most amino-terminated domain, is principally responsible for the high binding affinity to gp120, mainly using the C″ β-strand, with a gap between the D1 C′ strand and the gp120 surface.[52−54] It has been shown that sCD4 containing only the extracellular portion of the molecule retained high affinity binding to gp120 and was able to block the binding of HIV-1 to cell surface CD4 in vitro, thereby inhibiting infection of target cells.[52] The three-dimensional structure of the entire extracellular portion of sCD4 has been determined previously, and is shown in ribbon and space-filling models in Figure 3 and Figure S7 in the Supporting Information. The positions of the 39 lysines of sCD4 are identified in blue; most of the lysine residues were located on the surface of D1-D4 of sCD4 and therefore accessible for conjugation.[53,54]

To attach sCD4 to the external surface of the silica particles, the Npys group appended to the surface was cleaved with dithiothreitol (DTT) to yield a thiol-terminated surface, followed by reaction with the thiol-reactive maleimide heterobifunctional linker N-(β-maleimidopropyloxy)-succinimide ester (BMPS, Scheme 1). This created an external particle surface that was terminated with amine-reactive NHS esters; subsequent reaction with sCD4 led to surface

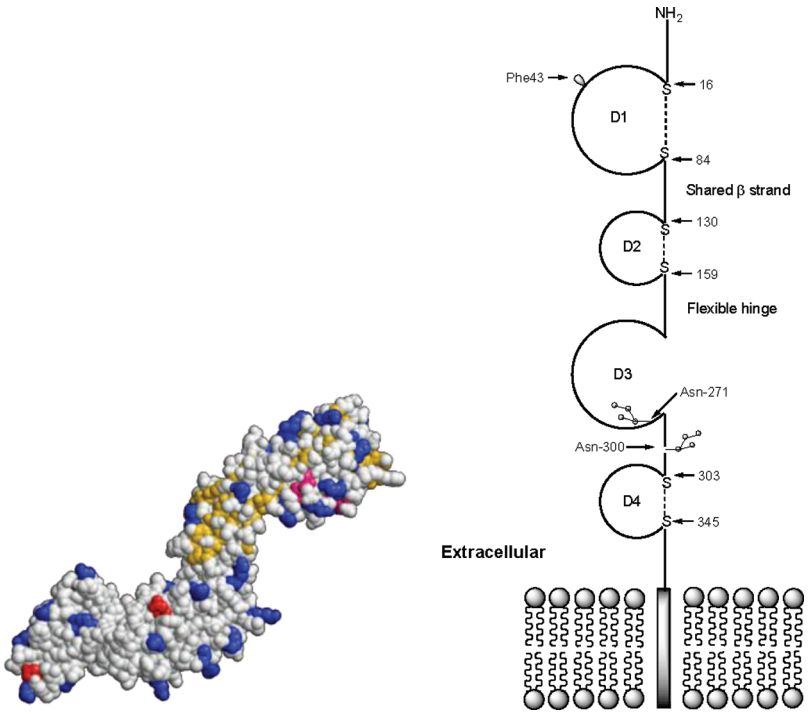

Figure 3. (a) Space-filling mode of four domains of sCD4, corresponding to recombinant soluble human CD4 residues 1−363. The backbone of the β-sheet secondary structures is shown in yellow, the side chains of lysine residues are shown in blue, and Asn271 and Asn300 are shown in red. The crystal coordinates were obtained from the RCSB Protein Data Bank (PDB ID: 1WIO). The image was constructed with RasTop (version 2.7). (b) Schematic representation of the major structural features of sCD4, including the D1-D4 immunoglobulin-like domains and the two Asn-linked oligosaccharide chains at Asn271 and Asn300. The cysteine residues involved in disulfide bonds are indicated by arrows together with their location in the amino acid sequence. Phe43, an important residue for gp120 binding, is also shown in the first domain.

immobilization through solvent-exposed lysines on the sCD4. However, because reaction could happen through any lysine, including those located near the gp120 binding region, this process could lead to a number of sCD4 molecules immobilized in a manner that prevented efficient binding. Other researchers have employed hydrazide binding as an appealing alternative conjugation method in which the carbohydrate moieties at well-defined glycoprotein sites far away from the affinity binding region can be employed.[55,56] Fortunately, sCD4 is glycosylated in the third domain (D3) at Asn271 and Asn300, but not the first domain (D1), which is responsible for gp120 binding. Previous work has indicated that forms of sCD4 with different glycans, or even deglycosylated sCD4, were still able to binds gp120 effectively.[57] The polysaccharide consists of fucose, *N*-acetylglucosamine, galactose, mannose, and sialic acid, where the sialic acid was easily converted to the aldehyde derivative by reaction with $NaIO_4$ to produce oxidized sCD4 ("ox-sCD4"). Separately, the thiol-terminated particles were reacted with *N*-(β-maleimidopropyloxy)hydrazide (BMPH), a heterobifunctional linker that produced a hydrazide-terminated surface. Reaction of the hydrazide-terminated particles with ox-sCD4 produced a solid that was attached to the external surface exclusively through the glycosidic linkage. We performed further characterization on these two types of particles (randomly bound sCD4 and specifically bound sCD4).

Thermodynamic and Kinetic Analysis of sCD4 Immobilization. The amount of sCD4 immobilized on the silica particles was monitored by the decrease in the absorbance of the supernatant at 595 nm using the Bradford assay.[58] As a non-specific control for the binding studies, we covalently immobilized bovine serum albumin (BSA) on APMS via amide coupling to yield APMS-BSA. BSA is the principal transporter of a wide variety of endogenous and exogenous compounds, and was conjugated to surfaces using the nonspecific lysine/NHS-ester reaction described above.[59] Kinetic curves of the immobilization of BSA, sCD4, and ox-sCD4 proteins on activated APMS are depicted in Figure 4. The effect of immobilization time on the coupling of the proteins to activated APMS samples was examined. For BSA and sCD4, $t_{1/2}$ for immobilization was ~60 min with more than 95% of maximum coverage achieved with ~4 h. However, immobilization of ox-sCD4 was much slower ($t_{1/2} \approx 120$ min). This is a reflection of the immobilization method for each material. Although BSA and sCD4 have many lysines available for conjugation, ox-sCD4 possesses only two oxidized carbohydrate chains for reaction with surface hydrazides. Additionally, hydrazide groups may be prevented from binding to ox-sCD4 because protein that has already been bound blocks additional protein from interacting with the surface. The latter concept could be tested by using smaller amounts of ox-sCD4 to obtain a lower surface coverage, to minimize mass transport effects for subsequent affinity binding tests.

When the plot of protein loading versus time shown in Figure 4a was taken out to longer times for for ox-CD4, there was no statistical difference from the saturation capacity shown in Table 1. Thus, for ease of comparison to the other two materials, data is shown up to $t = 6$ h. The saturation capacities of each protein on the various APMS samples could be examined by measuring the decrease in protein concentration after the addition of a series of functionalized particles under same conditions (Figure 4b). Plots of the protein concentration remaining in solution versus the amount of the APMS samples

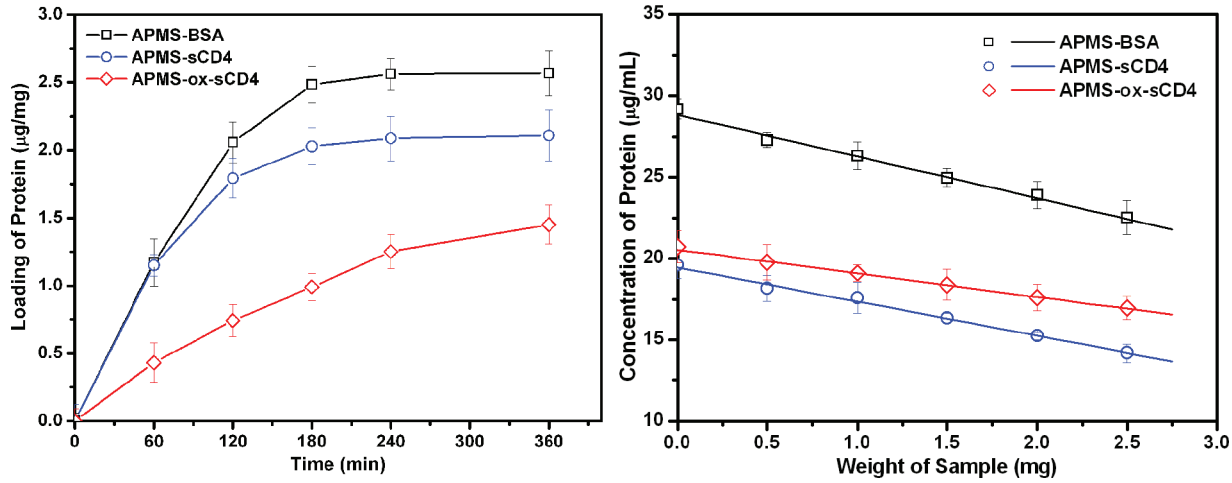

Figure 4. (a) Rates of immobilizations of BSA (black square) and sCD4 (blue circle) to NHS-ester-activated APMS and ox-sCD4 to hydrazide-activated APMS (red diamond). (b) Plots of saturation capacities for the materials in a.

Table 1. Saturation Capacities of Various APMS Samples for BSA, sCD4, and ox-sCD4

sample	protein	saturation capacity (μg/mg)	saturation capacity ($\times 10^{-11}$ mol/mg)
NHS-ester-activated APMS	BSA	2.56 ± 0.25	3.84 ± 0.37
NHS-ester-activated APMS	sCD4	2.10 ± 0.20	4.66 ± 0.33
hydrazide-activated APMS	ox-sCD4	1.45 ± 0.20	3.23 ± 0.33

consistently gave linear relationships, and the saturation capacities were obtained from the slopes of best-fit lines (Table 1); note that in the figure, lower protein concentration in solution (vertical axis) implies a higher amount of protein bound to the particle. Interestingly, the amount of immobilized protein was much smaller than the amount of available activated functional groups on each sample, suggesting that protein-surface coupling depended on the sizes of each immobilized protein. As shown in Figure 3, sCD4 has a rod-like shape (110 × 40 × 30 Å^3),[53] but the heart-shaped BSA molecule possesses a larger specific volume (80 × 70 × 60 Å^3) than sCD4.[59] Although sCD4 and ox-sCD4 show similar saturation capacity plots due to their similar sizes, a smaller amount of BSA was bound to the surface because of its larger specific volume.

Binding of HIV-1 gp120 Using Functionalized-APMS. Our overall goal was to develop modified particles for binding HIV gp120, for detection and purification applications. With CD4 peptide, sCD4, and ox-sCD4-modified silica particles in hand, we could now compare their relative performance in removal of gp120 from solution. After incubation of gp120 with functionalized mesoporous silica for 2 h, the particles were separated from the mixture via centrifugation and the amount of gp120 remaining in the residual supernatant was quantified using UV/vis spectroscopy. The easy separation of silica particles bound to the target molecule using centrifugation made the detection and quantification strategy fast, convenient, simple and easy. Quantification and kinetics of the gp120-binding process are shown in Figure 5a. It was found that half of the maximum amount of bound gp120 protein on each sample was obtained within about 2 h, with more than 95% of maximum coverage being achieved within 6 h. There was little difference in the rates of the affinity binding of gp120 to each sample, indicating that all forms of immobilized CD4 on the APMS samples were bound to gp120.[60] After the affinity binding reaction had reached completion (6 h), the maximum amount of the bound gp120 on each sample was obtained. The oxidized sCD4 protein, immobilized on the support through its oxidized carbohydrate residues was found to give the highest affinity for the gp120, whereas the 18-peptide CD4 fragment exhibited a relatively weak affinity for the gp120.

Saturation capacities for the binding affinity of HIV gp120 to a series of CD4- and sCD4-modified APMS were then examined. APMS-SH was used as a control. These particles were exposed to a solution containing either full-length gp120 glycoprotein or BSA for 6 h. In these tests, BSA is used as a nonspecific control, providing a qualitative estimate of nonspecific adsorption occurring in all samples. The saturation capacities of bound gp120 or BSA on each sample were calculated from the difference between the initial amounts and the amounts of the proteins remaining in solution after UV/Visible absorbance measurements. As shown in Figure 5b and Table 2, there were no significant differences in the abilities of APMS-SH, APMS-18-CD4 (2), APMS-sCD4 (3), or APMS-ox-sCD4 (4) to bind the negative protein control BSA (all modified APMS absorbed ≤0.3 μg of BSA/mg, presumably nonspecifically). In contrast, although APMS-SH showed no selectivity for gp120 over BSA, APMS-CD4 (2) captured nearly 3 times more gp120 than BSA. This indicated that even short peptide chains were selective for gp120 after surface immobilization, even if the capture efficiency was low. However, it was apparent that immobilization of whole sCD4 protein dramatically increased both the selectivity and capture efficiency for gp120. Furthermore, whole sCD4 protein immobilized through the carbohydrate chains had a significantly higher affinity for gp120 than when the same protein was randomly immobilized through lysine side chains. For example, as seen in Table 2, the stoichiometry of CD4-gp120 interaction on the APMS-ox-sCD4 was approximately 1:1, which is in quite good agreement with the other experimental results,[60−62] indicating that almost all of CD4 proteins retain their gp120 binding affinity even after being covalently immobilized to the silica surface. However, less than half of immobilized sCD4 on the APMS-sCD4 sample retained their binding affinity. Given numerous random couplings of the amine groups of the sCD4

dx.doi.org/10.1021/am2013008 | ACS Appl. Mater. Interfaces 2012, 4, 235−243

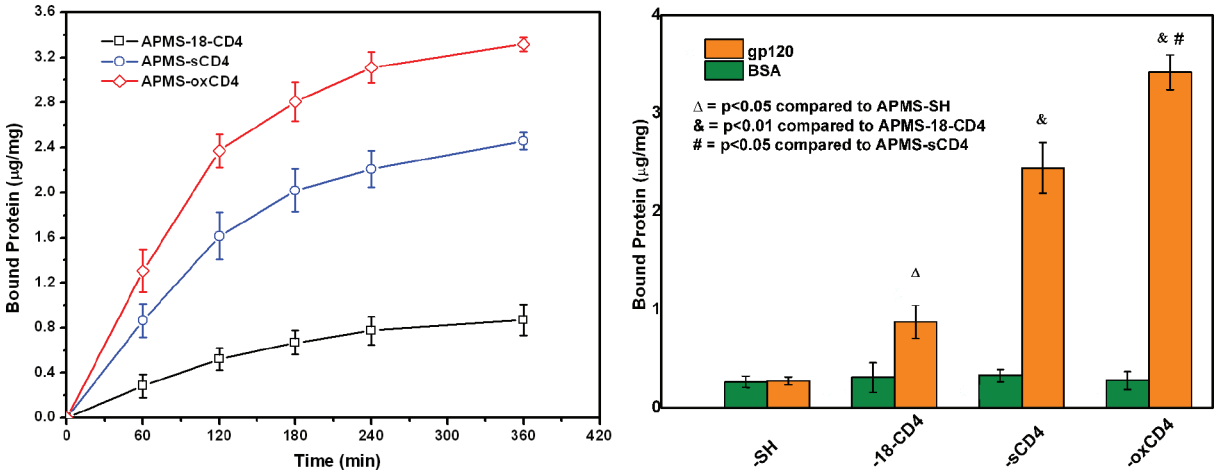

Figure 5. (a) Kinetic analysis of affinity binding of HIV gp120 to CD4 fragment or sCD4 protein immobilized on APMS samples. APMS-18CD4 (black square), APMS-sCD4 (blue circle), or APMS-ox-sCD4 (red diamond) were incubated at room temperature with 50 μg/mL gp120 in PBS. gp120 was assumed to have M_r = 110 000. (b) Saturation capacities of the binding affinity of HIV gp120 to the immobilized CD4 fragment or sCD4 proteins on APMS. Means ± SEM were calculated from at least three individual experiments.

Table 2. Comparison of BSA and gp120 Capture Efficiencies for Modified Silica Particles

	immobilized protein		bound BSA (μg/mg)			bound gp120		
Sample	(μg/mg)	($\times 10^{-11}$ mol/mg)	(μg/mg)	($\times 10^{-11}$ mol/mg)	BSA capture efficiency (%)	(μg/mg)	($\times 10^{-11}$ mol/mg)	gp120 capture efficiency (%)
APMS-**SH**			0.264 ± 0.056	0.396 ± 0.084		0.275 ± 0.039	0.250 ± 0.036	
APMS-**18-CD4**	52.8	2.79×10^6	0.311 ± 0.151	0.466 ± 0.226	**~0**	0.878 ± 0.167	0.798 ± 0.152	**~0**
APMS-**sCD4**	2.10 ± 0.20	4.66 ± 0.33	0.330 ± 0.066	0.495 ± 0.099	**10.6**	2.446 ± 0.258	2.224 ± 0.234	**47.7**
APMS-**oxCD4**	1.45 ± 0.20	3.23 ± 0.33	0.281 ± 0.093	0.421 ± 0.139	**13.0**	3.419 ± 0.177	3.108 ± 0.161	**96.2**

to the activated crosslinking molecule on the solid particle, the immobilization of sCD4 protein on the solid particles via the NHS-ester method could severely reduce its affinity binding for gp120 since there are several lysine residues in the first domain of CD4 required for gp120 binding affinity.[61] This nonspecific immobilization of the proteins involves random formation of amide linkages between the activated crosslinker and accessible amine groups on the proteins. Our system can be easily translated to in vivo delivery/imaging applications without the need to develop new detection system owing to the biocompatibility of mesoporous silica, targeting efficiency of immobilized sCD4 and encapsulating efficacy of potential drugs/contrast agents after pore "reopening".

Biological Implications of Molecular Conjugation by Polysaccharide-Linked Immobilization. The carbohydrate moieties of glycoproteins are known to play several important biological roles, mainly related to marking proteins for subsequent protection or modification or stabilizing bioactive conformations.[63] In viruses, carbohydrates have been implicated in biological activity, and in the maintenance of its overall structure.[64] Our results showed that conjugation of sCD4 via an oxidized carbohydrate chain does not affect binding to gp120. This is consistent with previously reported results showing that deglycosylation of sCD4 did not reduce its ability to bind gp120, proving that the carbohydrate is not necessary for binding.[65] This also confirms other observations in which cells expressing alerted or truncated forms of CD4 lacking the N-linked glycosylation sites were infected by HIV.[66] Importantly, deglycosylated gp120 and native gp120 have been shown to bind to CD4 receptors with comparable affinities, showing that the carbohydrate is not necessary for either protein to bind its partner.[65] This, however, cannot rule out the possible role of CD4 carbohydrate moieties in their effects on protein functions, neutralizing antibody response and mediating cellular adhesion.[67,68]

CONCLUSION

Several approaches were used to prepare porous silica particles functionalized with CD4 peptide fragments or whole sCD4 glycoprotein. The functional groups on the external surface of the particles were selectively activated for subsequent modification using a simple protection/deprotection strategy. Confirmation of the selective modification was provided by fluorescence CSLM, and the kinetics of peptide or glycoprotein modification was studied by UV/Vis spectroscopy. The results of a binding study using whole gp120 revealed that particles modified with an 18-peptide sequence surrounding Phe43, which is responsible for the majority of the contacts with gp120, were able to specifically bind and remove gp120 from solution, although to a significantly lower extent than particles modified with randomly oriented sCD4. These particles were in turn less effective at binding gp120 than sCD4 that had been specifically bound to the particles through its carbohydrate chain. These results showed that immobilization through oxidized sialic acids enabled CD4 to be attached to a solid surface in a homogeneous manner without loss of any gp120 binding affinity. Thus, our biodegradable mesoporous particles with surface-modified peptides/glycoproteins and accessible

dx.doi.org/10.1021/am2013008 | ACS Appl. Mater. Interfaces 2012, 4, 235–243

pore volumes represent a promising method for in vivo targeted detection/imaging and drug delivery to infected sites. This strategy could be also readily applied to a variety of particle-based therapies for diagnosis, drug encapsulation, gene transfection, bioimaging, or other applications.

EXPERIMENTAL METHODS

Preparation of HIV-gp120, sCD4, and CD4. Recombinant HIV-1 gp120 (LAV IIIB) external envelope protein, which is a full-length glycosylated recombinant protein derived from the *env* gene of HIV-1 (GenBank, M19921, NY5/BRU (LAV-1) recombinant clone pNL 4-3), was produced in insect cells using the baculovirus expression system, as with the gp 120 whose crystal structure was reported by Kwong et al.[26,69,70] The recombinant human soluble CD4 (sCD4), which is the full length glycosylated ectodomain, was produced using baculovirus vectors and secreted from insect cells in serum-free media. sCD4 is a 363-amino acid glycoprotein (~45 kDa) composed of four immunoglobulin-like domains (D1−D4). Both the recombinant gp120 and sCD4 were prepared, purified and characterized at Protein Sciences Corporation. Oligopeptides corresponding to residues 35−51 (KILGNQGSFLTKGPSKL) of T-cell surface glycoprotein CD4, was prepared under standard solid-phase synthesis conditions. **18-CD4** (C-KILGNQGSFLTKGPSKL) was prepared by incorporating cysteine at the *N*-terminus of the CD4 fragment in order to allow conjugation to APMS. The core of the CD4 fragment, residues 42−44 (C-SFL, b), and a lengthened CD4 fragment (4 alanines incorporated at both *N*-terminus and *C*-terminus of residues 35−51 of CD4 fragment, one cysteine residue was modified at C-terminus, AAAAKILGNQGSFLTKGPSKLAAAA-C, **26-CD4**) were synthesized similarly. In the syntheses of Cys-modified CD4 fragments (**4-CD4**, **18-CD4**, and **26-CD4**), 200 mg (140 μmol) of amino acid 2-Cl-Trt resin (0.7 mmol/g) was used. The *N*-Fmoc-amino acids, which had standard side-chain protective groups (Trt for Cys, Ser, Thr, Glu and Asn, Boc for Lys) were coupled to the peptide-resin as 1-benzotriazolyl (HOBt) esters. Coupling efficiency was monitored by the Kaiser method. The CD4 fragments were cleaved with TFA:triisopropylsilane (98.5:1.5) for 3 h yielding the corresponding requisite peptides as major components (~90% according to mass spectrum). After lyophilization, the peptides were purified by reverse-phase high-performance liquid chromatography (HPLC) on a LUNA C-18 column. The purities of the peptides were more than 95% as assessed by HPLC. The concentration of free thiol groups of these Cys-incorporated CD4 fragments were measured by spectrophotometric titration with 5,5′-dithiobis (2-nitrobenzoic acid) (Ellman's method).

CD4-Functionalized APMS and gp120 Binding Assay. Recombinant HIV-1 gp120 (LAV IIIB) solution was dialyzed against 10 mM PBS containing 150 mM NaCl at pH 7.4, and then diluted to 100 μg/mL with T-PBS buffer (10 mM PBS, 150 mM NaCl and 0.001% Tween 20, pH 7.4). The concentration of gp120 was initially determined by absorbance at 280 nm (ε_{280} = 0.74 mL cm^{-1} mg^{-1}), and subsequently determined by absorbance at 595 nm during binding experiments using a standard Bradford assay with an accuracy of ±10%. As a negative control, 30 μg/mL of bovine serum albumin (BSA) in 10 mM of PBS buffer was used as a reference (ε_{280} = 0.66 mL cm^{-1} mg^{-1}). The affinity binding experiments were performed at 25 °C in T-PBS buffer. 20.0 mg of various sCD4 or CD4 functionalized APMS was washed twice with 10 mM PBS buffer, filtered through a 0.45 μm filter, and then resuspended in 1.0 mL of the same PBS buffer. Aliquots (250 or 50 μL) of the suspensions (20 mg/mL) were transferred into centrifuge vials. The gp120 or BSA stock solutions were added into the suspensions to make the predetermined final concentration at 0.45 μM (50 μg/mL gp120 or 30 μg/mL BSA) in 0.5 mL of PBS buffer. After incubation at room temperature for 3 h with continuous shaking, centrifugation was applied, separating particle-bound protein. The supernatants were carefully removed, filtered through a 0.22 μm filter, and the residual protein concentrations was accurately measured at 595 nm using the Bradford microassay in a microplate microreader. Briefly, 150 μL of dye reagent (Coomassie Blue G250) were added to 150 μL of protein samples, and the mixtures were incubated at room temperature for ~5 min. The linear ranges of the assays for BSA or gp120 were 1−40 μg/mL. Finally, the amount of bound protein on each APMS sample was calculated from the difference of the initial and residual protein concentration (ΔA_{595}). Triplicate aliquots were assayed for each of the APMS samples. For the kinetic study, the supernatant of each mixture was obtained at predetermined time intervals followed by centrifugation and washing.

ASSOCIATED CONTENT

Supporting Information

Additional information, including complete synthetic details, full physical characterization of these and related materials, kinetic studies, and structural information for CD4 and gp120. This material is available free of charge via the Internet at http://pubs.acs.org.

AUTHOR INFORMATION

Corresponding Author

*E-mail: christopher.landry@uvm.edu. Fax: +1 802 656 8705.

ACKNOWLEDGMENTS

We thank Prof. Douglas Taatjes of the Medical Imaging Center for advice and assistance in obtaining confocal images.

REFERENCES

(1) Vallet-Regi, M. A.; Ruiz-Gonzalez, L.; Izquierdo-Barba, I.; Gonzalez-Calbet, J. M. *J. Mater. Chem.* **2006**, *16*, 26−31.
(2) Cheng, K.; Blumen, S. R.; Weiss, D. J.; James, T. A.; Mossman, B. T.; Landry, C. C. *ACS Appl. Mater. Interfaces* **2010**, *2*, 2489−2495.
(3) Rosenholm, J.; Sahlgren, C.; Linden, M. *J. Mater. Chem.* **2010**, *20*, 2707−2713.
(4) Rosenholm, J. M.; Peuhu, E.; Eriksson, J. E.; Sahlgren, C.; Linden, M. *Nano Lett.* **2009**, *9*, 3308−3311.
(5) Lu, C. W.; Hung, Y.; Hsiao, J. K.; Yao, M.; Chung, T. H.; Lin, Y. S.; Wu, S. H.; Hsu, S. C.; Liu, H. M.; Mou, C. Y.; Yang, C. S.; Huang, D. M.; Chen, Y. C. *Nano Lett.* **2007**, *7*, 149−154.
(6) Steinbacher, J. L.; Lathrop, S. A.; Cheng, K.; Hillegass, J. M.; Kauppinen, R. A.; Mossman, B. T.; Landry, C. C. *Small* **2010**, *6*, 2678−2682.
(7) Zhan, Q. Q.; Qian, J.; Li, X.; He, S. L. *Nanotechnology* **2010**, *21*, 055704.
(8) Hillegass, J. M.; Blumen, S. R.; Cheng, K.; MacPherson, M. B.; Alexeeva, V.; Lathrop, S. A.; Beuschel, S. L.; Steinbacher, J. L.; Butnor, K. J.; Ramos-Niño, M. E.; Shukla, A.; James, T. A.; Weiss, D. J.; Taatjes, D. J.; Pass, H. I.; Carbone, M.; Landry, C. C.; Mossman, B. T. *Int. J. Cancer* **2011**, *129*, 233.
(9) Vivero-Escoto, J. L.; Slowing, II; Trewyn, B. G.; Lin, V. S. Y. *Small* **2010**, *6*, 1952−1967.
(10) Rosenholm, J. M.; Sahlgren, C.; Linden, M. *Nanoscale* **2010**, *2*, 1870−1883.

(11) Livingston, S. R.; Landry, C. C. *J. Am. Chem. Soc.* **2008**, *130*, 13214−13215.
(12) Liong, M.; France, B.; Bradley, K. A.; Zink, J. I. *Adv. Mater.* **2009**, *21*, 1684.
(13) Yang, H. H.; Zhang, S. Q.; Chen, X. L.; Zhuang, Z. X.; Xu, J. G.; Wang, X. R. *Anal. Chem.* **2004**, *76*, 1316−1321.
(14) Qian, K.; Wan, J. J.; Huang, X. D.; Yang, P. Y.; Liu, B. H.; Yu, C. Z. *Chem.—Eur. J.* **2010**, *16*, 822−828.
(15) Zhang, L. J.; Xu, Y. W.; Yao, H. L.; Xie, L. Q.; Yao, J.; Lu, H. J.; Yang, P. Y. *Chem.—Eur. J.* **2009**, *15*, 10158−10166.
(16) Zhang, L. J.; Lu, H. J.; Yang, P. Y. *Sci. China Chem.* **2010**, *53*, 695−703.
(17) Liu, S. S.; Chen, H. M.; Lu, X. H.; Deng, C. H.; Zhang, X. M.; Yang, P. Y. *Angew. Chem. Int. Ed.* **2010**, *49*, 7557−7561.
(18) Wan, J. J.; Qian, K.; Zhang, J.; Liu, F.; Wang, Y. H.; Yang, P. Y.; Liu, B. H.; Yu, C. Z. *Langmuir* **2010**, *26*, 7444−7450.
(19) Xu, Y. W.; Wu, Z. X.; Zhang, L. J.; Lu, H. J.; Yang, P. Y.; Webley, P. A.; Zhao, D. Y. *Anal. Chem.* **2009**, *81*, 503−508.
(20) El-Boubbou, K.; Gruden, C.; Huang, X. *J. Am. Chem. Soc.* **2007**, *129*, 13392−13393 and references therein.
(21) El-Boubbou, K.; Zhu David, C.; Vasileiou, C.; Borhan, B.; Prosperi, D.; Li, W.; Huang, X. *J. Am. Chem. Soc.* **2010**, *132*, 4490−9.
(22) Kim, E. Y.; Stanton, J.; Korber, B. T.; Krebs, K.; Bogdan, D.; Kunstman, K.; Wu, S.; Phair, J. P.; Mirkin, C. A.; Wolinsky, S. M. *Nanomedicine* **2008**, *3*, 293.
(23) Tang, S. X.; Hewlett, I. *J. Infect. Dis.* **2010**, *201*, S59−S64.
(24) Tang, S. X.; Zhao, J. Q.; Storhoff, J. J.; Norris, P. J.; Little, R. F.; Yarchoan, R.; Stramer, S. L.; Patno, T.; Domanus, M.; Dhar, A.; Mirkin, C. A.; Hewlett, I. K. *J. Acquired Immune Defic. Syndr.* **2007**, *46*, 231−237.
(25) Myszka, D. G.; Sweet, R. W.; Hensley, P.; Brigham-Burke, M.; Kwong, P. D.; Hendrickson, W. A.; Wyatt, R.; Sodroski, J.; Doyle, M. L. *Proc. Natl. Acad. Sci.* **2000**, *97*, 9026−9031.
(26) Kwong, P. D.; Wyatt, R.; Robinson, J.; Sweet, R. W.; Sodroski, J.; Hendrickson, W. A. *Nature* **1998**, *393*, 648−659.
(27) Wyatt, R.; Kwong, P. D.; Desjardins, E.; Sweet, R. W.; Robinson, J.; Hendrickson, W. A.; Sodroski, J. G. *Nature* **1998**, *393*, 705−711.
(28) Chen, L.; Kwon, Y. D.; Zhou, T. Q.; Wu, X. L.; O'Dell, S.; Cavacini, L.; Hessell, A. J.; Pancera, M.; Tang, M.; Xu, L.; Yang, Z. Y.; Zhang, M. Y.; Arthos, J.; Burton, D. R.; Dimitrov, D. S.; Nabel, G. J.; Posner, M. R.; Sodroski, J.; Wyatt, R.; Mascola, J. R.; Kwong, P. D. *Science* **2009**, *326*, 1123−1127.
(29) Diskin, R.; Marcovecchio, P. M.; Bjorkman, P. J. *Nat. Struct. Mol. Biol.* **2010**, *17*, 608−613.
(30) Wang, J. H.; Alvarez, R.; Roderiquez, G.; Guan, E.; Norcross, M. A. *J. Cell. Biochem.* **2004**, *93*, 753−760.
(31) Xiao, X. D.; Wu, L. J.; Stantchev, T. S.; Feng, Y. R.; Ugolini, S.; Chen, H.; Shen, Z. M.; Riley, J. L.; Broder, C. C.; Sattentau, Q. J.; Dimitrov, D. S. *Proc. Natl. Acad. Sci.* **1999**, *96*, 7496−7501.
(32) Dragic, T.; Litwin, V.; Allaway, G. P.; Martin, S. R.; Huang, Y. X.; Nagashima, K. A.; Cayanan, C.; Maddon, P. J.; Koup, R. A.; Moore, J. P.; Paxton, W. A. *Nature* **1996**, *381*, 667−673.
(33) (a) Karlsson Hedestam, G. B.; Fouchier, R. A. M.; Phogat, S.; Burton, D. R.; Sodroski, J.; Wyatt, R. T. *Nat. Rev.* **2008**, *6*, 143. (b) Bhattacharyya, S.; Rajan, R. E.; Swarupa, Y.; Rathore, U.; Verma, A.; Udaykumar, R.; Varadarajan, R. *J. Biol. Chem.* **2010**, *285*, 27100.
(34) Lagenaur, L. A.; Villarroel, V. A.; Bundoc, V.; Dey, B.; Berger, E. A. *Retrovirology* **2010**, *7*, 1−13.
(35) Vinu, A.; Hossain, K. Z.; Ariga, K. *J. Nanosci. Nanotechnol.* **2005**, *5*, 347.
(36) Liu, Y.-H.; Lin, H.-P.; Mou, C.-Y. *Langmuir* **2004**, *20*, 3231.
(37) Huh, S.; Wiench, J. W.; Yoo, J.-C.; Pruski, M.; Lin, V. S.-Y. *Chem. Mater.* **2003**, *15*, 4247.
(38) Mal, N.-K.; Fujiwara, M.; Tanaka, Y. N. *Nature* **2003**, *421*, 350−353.
(39) Cheng, K. Ph.D. Thesis, University of Vermont: Burlington, 2007.
(40) Gallis, K. W.; Araujo, J. T.; Duff, K. J.; Moore, J. G.; Landry, C. C. *Adv. Mater.* **1999**, *11*, 1452.
(41) Gallis, K. W.; Landry, C. C. U.S. Patent 6 334 988, 2002.
(42) Gallis, K. W.; KEklund, A. G.; Jull, S. T.; Araujo, J. T.; Moore, J. G.; Landry, C. C. *Stud. Surf. Sci. Catal.* **2000**, *129*, 747.
(43) Nassivera, T. W.; Eklund, A. G.; Landry, C. C. *J. Chromatogr., A* **2002**, *973*, 97.
(44) Sorensen, A. C.; Fuller, B. L.; Eklund, A. G.; Landry, C. C. *Chem. Mater.* **2004**, *16*, 2157.
(45) Cheng, K.; Landry, C. C. *J. Am. Chem. Soc.* **2007**, *129*, 9674−9685.
(46) Jameson, B. A.; Rao, P. E.; Kong, L. I.; Hahn, B. H.; Shaw, G. M.; Hood, L. E.; Kent, S. B. H. *Science* **1988**, *240*, 1335−1339.
(47) Gizachew, D.; Moffett, D. B.; Busse, S. C.; Westler, W. M.; Dratz, E. A.; Teintze, M. *Biochemistry* **1998**, *37*, 10616−10625.
(48) Houseman, B. T.; Gawalt, E. S.; Mrksich, M. *Langmuir* **2003**, *19*, 1522−1531.
(49) Miyazawa, T.; Blout, E. R. *J. Am. Chem. Soc.* **1961**, *83*, 712−719.
(50) Henkel, B.; Bayer, E. *J. Pept. Sci.* **1998**, *4*, 461−470.
(51) Haris, P. I.; Chapman, D.; Harrison, R. A.; Smith, K. F.; Perkins, S. J. *Biochemistry* **1990**, *29*, 1377−1380.
(52) Chamow, S. M.; Kogan, T. P.; Peers, D. H.; Hastings, R. C.; Byrn, R. A.; Ashkenazi, A. *J. Biol. Chem.* **1992**, *267*, 15916−15922.
(53) Ryu, S. E.; Kwong, P. D.; Truneh, A.; Porter, T. G.; Arthos, J.; Rosenberg, M.; Dai, X. P.; Xuong, N. H.; Axel, R.; Sweet, R. W.; Hendrickson, W. A. *Nature* **1990**, *348*, 419−426.
(54) Harris, R. J.; Chamow, S. M.; Gregory, T. J.; Spellman, M. W. *Eur. J. Biochem.* **1990**, *188*, 291−300.
(55) Rodwell, J. D.; Alvarez, V. L.; Chyi, L.; Lopes, A. D.; Goers, J. W. F.; King, H. D.; Powsner, H. J.; Mckearn, T. J. *Proc. Natl. Acad. Sci.* **1986**, *83*, 2632−2636.
(56) Xuan, H.; Hage, D. S. *Anal. Biochem.* **2005**, *346*, 300−310.
(57) (a) Morikawa, Y.; Overton, H. A.; Moore, J. P.; Wilkinson, A. J.; Brady, R. L.; Lewis, S. J.; Jones, I. M. *AIDS Res. Hum. Retroviruses* **1990**, *6*, 765. (b) Fenouillet, E.; Clergetraslain, B.; Gluckman, J. C.; Guetard, D.; Montagnieri, L.; Bahraouit, E. *J. Exp. Med.* **1989**, *169*, 802. (c) Ashford, D. A.; Alafi, C. D.; Gamble, V. M.; Mackay, D. J. G.; Rademacher, T. W.; Williams, P. J.; Dwek, R. A.; Barclay, A. N.; Davis, S. J.; Somoza, C.; Ward, H. A.; Williams, A. F. *J. Biol. Chem.* **1993**, *268*, 3260.
(58) Bradford, M. *Anal. Biochem.* **1976**, *72*, 248−254.
(59) Huang, B. X.; Kim, H. Y.; Dass, C. *J. Am. Soc. Mass Spectrom* **2004**, *15*, 1237−1247.
(60) Myszka, D. G.; Sweet, R. W.; Hensley, P.; Brigham-Burke, M.; Kwong, P. D.; Hendrickson, W. A.; Wyatt, R.; Sodroski, J.; Doyle, M. L. *Proc. Natl. Acad. Sci.* **2000**, *97*, 9026−9031.
(61) Chamow, S. M.; Kogan, T. P.; Peers, D. H.; Hastings, R. C.; Byrn, R. A.; Ashkenazi, A. *J. Biol. Chem.* **1992**, *267*, 15916−15922.
(62) Wu, H.; Myszka, D. G.; Tendian, S. W.; Brouillette, C. G.; Sweet, R. W.; Chaiken, I. M.; Hendrickson, W. A. *Proc. Natl. Acad. Sci.* **1996**, *93*, 15030−15035.
(63) Bertozzi, C. R.; Kiessling, L. L. *Science* **2001**, *291*, 2357−2364.
(64) Papandreou, M. J.; Idziorek, T.; Miquelis, R.; Fenouillet, E. *FEBS Lett.* **1996**, *379*, 171−176.
(65) Fenouillet, E.; Clergetraslain, B.; Gluckman, J. C.; Guetard, D.; Montagnier, L.; Bahraoui, E. *J. Exp. Med.* **1989**, *169*, 807−822.
(66) Bedinger, P.; Moriarty, A.; von Borstel, R. C.; Donovan, N. J.; Steimer, K. S.; Littman, D. R. *Nature* **1988**, *334*, 162−165.
(67) Koch, M.; Pancera, M.; Kwong, P. D.; Kolchinsky, P.; Grundner, C.; Wang, L. P.; Hendrickson, W. A.; Sodroski, J.; Wyatt, R. *Virology* **2003**, *313*, 387−400.
(68) Quinones-Kochs, M. I.; Buonocore, L.; Rose, J. K. *J. Virol.* **2002**, *76*, 4199−4211.
(69) Kwong, P. D.; Wyatt, R.; Desjardins, E.; Robinson, J.; Culp, J. S.; Hellmig, B. D.; Sweet, R. W.; Sodroski, J.; Hendrickson, W. A. *J. Biol. Chem.* **1999**, *274*, 4115−23.
(70) Culp, J. S.; Johansen, H.; Hellmig, B.; Beck, J.; Matthews, T. J.; Delers, A.; Rosenberg, M. *Nat. Biotechnol.* **1991**, *9*, 173−177.